Heliyon 10 (2024) e37475

Contents lists available at ScienceDirect

Heliyon

journal homepage: www.cell.com/heliyon

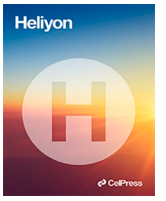

Research article

Light-phase time-restricted feeding disrupts the muscle clock and insulin sensitivity yet potentially induces muscle fiber remodeling in mice

Zhou Ye [a,1], Kai Huang [f,1], Xueqin Dai [c], Dandan Gao [d], Yue Gu [e], Jun Qian [a], Feng Zhang [b,**], Qiaocheng Zhai [a,b,e,*]

[a] Division of Spine Surgery, The Quzhou Affiliated Hospital of Wenzhou Medical University, Quzhou People's Hospital, Quzhou, China
[b] The Joint Innovation Center for Engineering in Medicine, The Quzhou Affiliated Hospital of Wenzhou Medical University, Quzhou People's Hospital, Quzhou, China
[c] Jiangsu Key Laboratory of Neuropsychiatric Diseases, Institute of Neuroscience, Soochow University, Suzhou, China
[d] Wenzhou Medical University, Wenzhou, China
[e] Jiangsu Key Laboratory of Neuropsychiatric Diseases and Cambridge-Su Genomic Resource Center, Medical School of Soochow University, Suzhou, China
[f] Orthopaedic Institute, Wuxi 9th People's Hospital Affiliated to Soochow University, Wuxi, China

ARTICLE INFO

Keywords:
Time-restricted feeding
Skeletal muscle
Circadian clock
Muscle fiber remodeling
Bone mass

ABSTRACT

Skeletal muscle plays a critical role in regulating systemic metabolic homeostasis. It has been demonstrated that time-restricted feeding (TRF) during the rest phase can desynchronize the suprachiasmatic nucleus (SCN) and peripheral clocks, thereby increasing the risk of metabolic diseases. However, the impact of dietary timing on the muscle clock and health remains poorly understood. Here, through the analysis of cycling genes and differentially expressed genes in the skeletal muscle transcriptome, we identified disruptions in muscle diurnal rhythms by 2 weeks of light-phase TRF. Furthermore, compared with ad libitum (AL) feeding mice, 2 weeks of light-phase TRF was found to induce insulin resistance, muscle fiber type remodeling, and changes in the expression of muscle growth-related genes, while both light-phase and dark-phase TRF having a limited impact on bone quality relative to AL mice. In summary, our research reveals that the disruption of the skeletal muscle clock may contribute to the abnormal metabolic phenotype resulting from feeding restricted to the inactive period. Additionally, our study provides a comprehensive omics atlas of the diurnal rhythms in skeletal muscle regulated by dietary timing.

* Corresponding author. Division of Spine Surgery, The Quzhou Affiliated Hospital of Wenzhou Medical University, Quzhou People's Hospital, No. 100 Minjiang Avenue, Quzhou, 324100, China.
** Corresponding author. The Joint Innovation Center for Engineering in Medicine, The Quzhou Affiliated Hospital of Wenzhou Medical University, Quzhou People's Hospital, No. 100 Minjiang Avenue, Quzhou, 324100, China.
E-mail addresses: fengzhang@wmu.edu.cn (F. Zhang), zhaiqiaocheng@wmu.edu.cn (Q. Zhai).
[1] These authors contributed equally to this work and share first authorship.

https://doi.org/10.1016/j.heliyon.2024.e37475
Received 8 May 2024; Received in revised form 3 September 2024; Accepted 4 September 2024
Available online 14 September 2024

1. Introduction

For the circadian pacemaker, the suprachiasmatic nucleus (SCN), can be entrained by light-dark cycles and orchestrates the peripheral clocks, which operate with a cycle of approximately 24 h. This coordination regulates various physiological activities, including sleep-wake cycles, feeding, body temperature, and hormone secretion [1]. At the molecular level, the circadian clock is governed by a transcriptional translation feedback loop (TTFL) [2]. Within this system, the heterodimer composed of BMAL1 and CLOCK binds to the E-box element, thereby regulating the expression of clock-controlled genes such as *Per* and *Cry*. Subsequently, the PER and CRY proteins undergo phosphorylation in the cytoplasm and translocate to the nucleus to inhibit the transcriptional activation activity of the BMAL1 and CLOCK heterodimer. Additionally, REV-ERBs and RORs play roles in inhibiting and activating the transcription of *Bmal1*, creating a secondary feedback loop for circadian clock regulation.

Time-restricted feeding (TRF) involves limiting food intake to a specific time window, typically lasting 4–12 h, without caloric restriction. This dietary approach has demonstrated significant metabolic benefits when applied during the active phase [3]. TRF during the active phase has been shown to mitigate obesity induced by high-fat diets, improve myocardial contractile function in mice [4–6], and counteract age-related heart failure and muscle function disruption caused by high-fat diets in fruit flies [7,8]. It is reported that early TRF can improve insulin sensitivity, blood pressure, and oxidative stress in men with prediabetes [9]. Additionally, a 10-h TRF can improve cardiometabolic health and quality of life in shift-workers [10]. These findings suggest that TRF can serve as a non-pharmacological intervention for treating metabolism-related diseases in both animal models and humans. However, when food intake occurs during the rest phase, as often happens with shift workers and those who eat late at night, it can reset peripheral clocks and lead to circadian desynchronization between the SCN and peripheral tissues [11,12]. This desynchronization has been linked to metabolic diseases [13,14]. Skeletal muscle, which constitutes about 40 % of an individual's body mass, plays a crucial role in sports performance, metabolic homeostasis [15], and bone health [16]. Disrupting the skeletal muscle clock, as seen in *Bmal1* knockout models, results in impaired insulin-stimulated glucose uptake [17], muscle fiber remodeling, and premature aging characteristics, including increased bone calcification and reduced joint collagen [18]. Thus, investigating the effects of TRF on the skeletal muscle clock may unveil a novel mechanism contributing to metabolic diseases resulting from unhealthy eating habits.

A recent study found that a 2-h calorie restricted feeding can increase the lifespan of C57 mice, and the improvement of lifespan by a restricted feeding at ZT12-14 is stronger than that by a restricted feeding at ZT0-2 (ZT: circadian time under 12 h:12 h light–dark cycles, ZT0 refers to lights on), indicating that the body's physiological homeostasis is time-dependent in response to the time signal of eating [19]. In our previous research, we set 12 different 4-h TRF phases in a 24-h day and used the wheel running rhythm as the output indicator of the circadian clock to map the phase response curve of C57 mice to dietary signals. Our study showed that ZT0-4 TRF can reprogram the SCN transcriptome and calcium rhythms. Furthermore, it leads to enduring changes in the wheel-running behavior of mice through IGF2-KCC2 pathway in the SCN [20]. However, our study only focused on the effect of TRF on the SCN, and the impact of TRF on the skeletal muscle system that regulates motor function remains unclear. Therefore, this study aims to explore the regulation of the skeletal muscle clock and physiological homeostasis induced by ZT0-4 TRF.

2. Materials and methods

2.1. Animals

6–8 weeks old C57BL/6J mice (Gempharmatech Co., Ltd) were housed in specific-pathogen-free facilities with free access to normal chow diet (ShooBree SPF Mice Diet, 28 % protein, 13 % fat, 57 % carbohydrates) and water under the 12 h:12 h light–dark (LD) cycles. Male mice were adapted to LD for 2 weeks, followed by 4 h of TRF at ZT0-4 or Ad libitum (control) for two weeks. For the experiment exploring the effect of TRF on bone quality, we included an experimental group of ZT12-16 TRF. During TRF, all cage changes were performed during both the food introduction and food withdrawal periods [20]. All animal procedures were approved by the Animal Care and Use Committee of the CAM-SU Genomic Resource Center, Soochow University (YX-2018-4). The wheel-running activity was recorded and analyzed using ClockLab (Actimetrics, Evanston, IL).

2.2. RNA-seq

After two weeks of ZT0-4 TRF, mice were released to constant darkness with free access to food, and then mice were sacrificed after 24 h at CT1, CT7, CT13 and CT19, gastrocnemius muscle samples were collected (N = 3 per time point). The gastrocnemius muscle is quick-frozen with liquid nitrogen and stored in a −80 °C refrigerator. After adding 1 mL of Trizol to the sample, the tissue is lysed using a high-throughput tissue grinder, followed by RNA extraction.

RNA-seq was performed on an Illumina NovaSeq 6000 platform at the Genewiz, Suzhou, China. Cuffdiff v1.3.0 was used to calculate FPKMs for genes. DESeq2 was used to identify differentially expressed genes with $P < 0.05$ and fold changes ≥ 2.

2.3. Identification of cycling genes

The RAIN [21] and Metacycle [22] were used to identify cycling genes based on the FPKM data with 4 time points. The overlapped genes of RAIN and Metacycle were used for further analysis. $P < 0.05$ was considered significant. The phase, amplitude for each transcript of cycling genes were also calculated with Metacycle.

2.4. Q-PCR

The RNA concentration of the gastrocnemius was determined by a NanoDrop (Thermo), and the cDNA was synthesized using a NovoScript Plus All-in-one 1st Strand cDNA Synthesis SuperMix (Novoprotein). Quantitative real-time PCR was performed using NovoStart SYBR qPCR SuperMix plus (Novoprotein) with StepOne Plus (Applied Biosystems). The relative levels of *Bmal1*, *Clock*, *Per1*, *Per2*, *Cry1*, *Cry2* and *Nr1d1* were normalized to *Gapdh*. Primer information for Q-PCR is included in Table S1.

2.5. Western blot

Immediately after the mice were sacrificed, the gastrocnemius muscles were quickly frozen in liquid nitrogen and stored in a −80 °C refrigerator. To extract gastrocnemius muscle protein, gastrocnemius muscle was powdered within liquid nitrogen and collected in EP tubes. 500 μL RIPA lysis buffer containing protease and phosphatase inhibitors was added, and kept on ice for 30 min. After centrifugation at 4 °C and 13000 rpm for 10 min, supernatant was collected. The BCA method was used to determine the protein concentration. After SDS-PAGE electrophoresis, the protein was transferred to a PVDF membrane, then blocked with 5 % milk or BSA. Membranes were incubated with primary antibodies (MYH1: proteintech 25182-1-AP 1:1000, MYH2: proteintech 66212-1-Ig 1:5000, MYH4: proteintech 20140-1-AP 1:1000, MYH7: proteintech 22280-1-AP 1:1000, Tubulin: proteintech 11224-1-AP 1:3000, GAPDH: proteintech 60004-1-Ig 1:3000, p-AKT: proteintech 66444-1-Ig 1:2000, AKT: CST 9272S 1:1000) overnight at 4 °C. After being washed three times with TBST, membranes were incubated with secondary antibodies (proteintech SA00001-1 1:10000, proteintech SA00001-2 1:10000) at room temperature for 1 h. Membranes were then visualized with a chemiluminescence imager (Tannon). Use ImageJ software for protein quantification.

2.6. ITT/GTT

AL and ZT0-4 TRF mice were subjected to an insulin tolerance test (ITT) experiment after 6 h of fasting (ZT10) on 14th day of TRF under LD condition. The mice were weighed, and injected intraperitoneally with insulin at a dose of 1 U/kg, blood glucose was measured at 0, 15, 30, 60, 90, and 120 min after the injection [23].

After TRF mice were released to AL feeding, both AL and TRF mice were fasted overnight before glucose tolerance test (GTT) experiments. The mice were weighed, and injected intraperitoneally with glucose at a dose of 2 g/kg under LD condition at ZT0. Blood glucose was measured and recorded at 0, 15, 30, 60, 90, and 120 min after injection [24].

2.7. Immunofluorescence

Fresh mouse muscles were put into isopentane and quickly frozen using liquid nitrogen. The samples were embedded using OCT and the muscle tissue was cut into 6 μm sections. The frozen sections were fixed with 4 % paraformaldehyde for 15 min and then washed twice with PBS. Then, 0.3 % Triton was added to the sections for permeabilization at room temperature for 15 min. After blocking the sections with 10 % normal goat serum in PBS at room temperature for 1 h, MYH4 (proteintech 20140-1-AP) and MYH7 (proteintech 22280-1-AP) antibodies were added at a ratio of 1:400 and incubated overnight at 4 °C. The next day, the primary antibody was washed and Alexa Fluor™ 594 (invitrogen R37117) was added and incubated at room temperature for 1 h, and scanned using a Pannoramic Slide Scanner. The percentage of muscle fiber area was analyzed using imageJ.

2.8. micro-CT

The unilateral femurs of mice were fixed using 4 % PFA, and then transferred to 70 % alcohol for storage. Samples were scanned using a micro-CT scanner (Bruker SkyScan 1176) at 50 KV, 500 μA, 1000 ms with a 9 μm voxel size. For trabecular measurements, a region of interest of 1.75 mm length starting from 540 μm proximal to the distal growth plate was analyzed. Microstructural parameters of the bone were calculated, including bone mineral density (BMD, g/cm^3), bone volume fraction (BV/TV, %), trabecular bone thickness (Tb. Th, mm), trabecular number (Tb. N, 1/mm), and trabecular separation (Tb. Sp, mm). Materialise Magics 24.0 software was used to generate visualizations for the reconstructed cortical bone and trabecular bone.

2.9. Statistical analysis

The statistical analyses were performed using Student's *t*-tests in GraphPad Prism 8. For micro-CT results, we utilized one-way ANOVA to analyze the differences among the AL, ZT0-4 TRF and ZT12-16 TRF groups. Two-way ANOVA was used to analyze the time series data, including clock genes expression and food intake. $P < 0.05$ was considered statistically significant ($^*P < 0.05$, $^{**}P < 0.01$, and $^{***}P < 0.001$).

3. Results

3.1. Disruption of the muscle clock by ZT0-4 TRF

Our study found that compared with AL mice, ZT0-4 TRF increased the subjective daytime activity time of mice in constant

darkness (Figs. S1A and S1B). To investigate the influence of ZT0-4 TRF on the circadian clock of skeletal muscle, we conducted RAIN and Metacycle analysis using transcriptome data of gastrocnemius muscle collected at CT1, CT7, CT13, and CT19 (CT: circadian time under constant darkness) 24 h after ZT0-4 TRF. The analysis revealed that in ad libitum (AL) mice, there were 1948 cycling genes (Table S2), while the number of cycling genes in the ZT0-4 TRF group reduced to 740 (Table S3), with only 154 genes maintaining their rhythmicity in both AL and TRF groups (Fig. 1A and B). When assessing the amplitude of cycling genes, we observed that the medium amplitude of AL cycling genes exceeded that of TRF cycling genes (0.1559 vs. 0.1509) (Fig. 1C). Furthermore, ZT0-4 TRF induced a shift in the phase of cycling genes, with the rhythm genes in the AL group primarily concentrated in CT0-6, while those in the TRF group were primarily concentrated in CT12-18 (Fig. 1D).

To determine if the reduction in the number and amplitude of TRF-induced cycling genes correlated with changes in the expression of core clock genes, we analyzed the expression of these genes in muscle. We found that comparing with AL mice, the amplitudes of *Bmal1, Clock, Per1, Per2, Cry1, Cry2, Nr1d1,* and *Dbp* in TRF mice were significantly reduced, and the rhythmic expression of *Bmal1, Clock, Cry1,* and *Cry2* nearly disappeared (Fig. 1E). Furthermore, we detected the expression of the above core clock genes through Q-

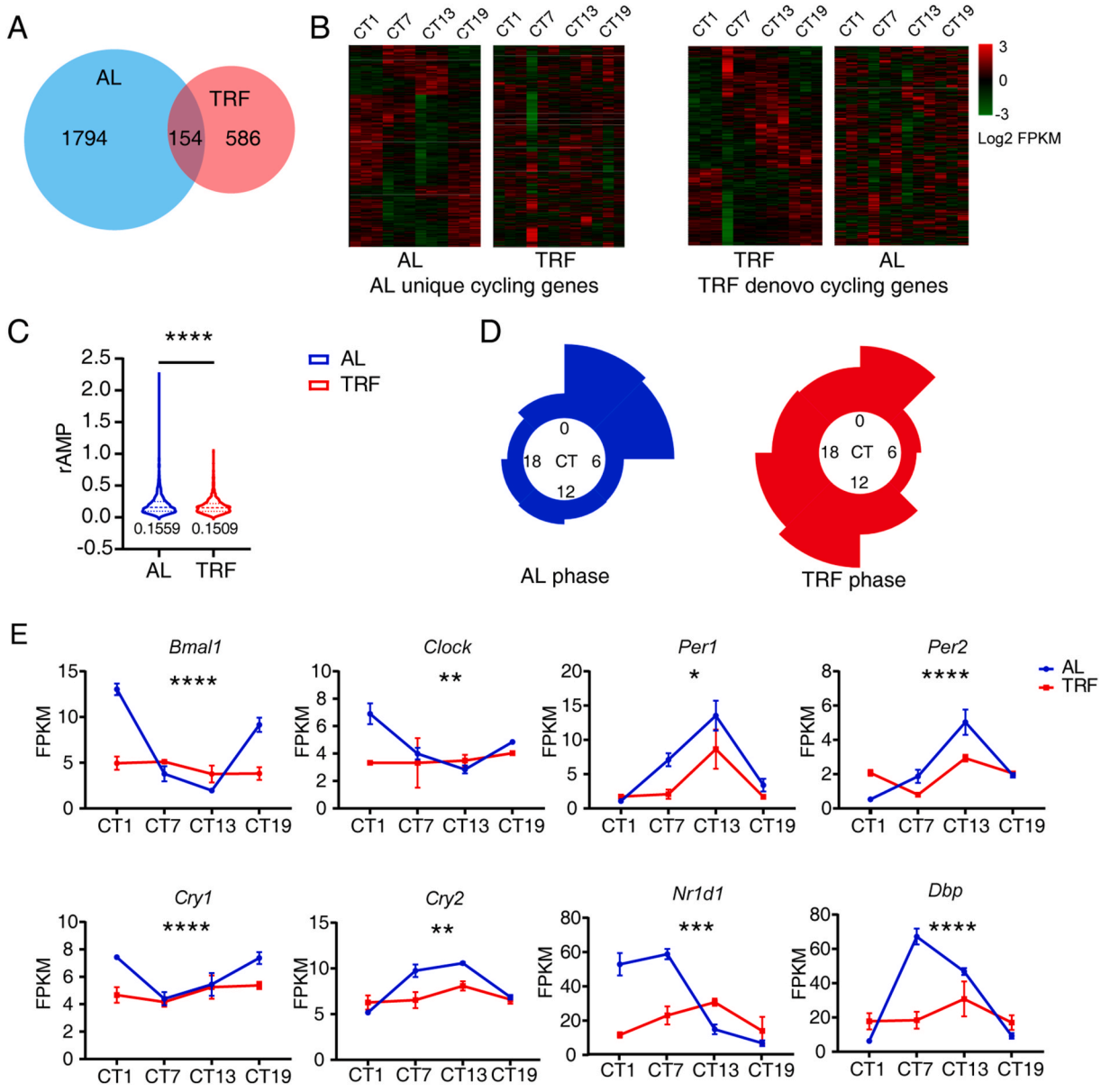

Fig. 1. ZT0-4 TRF disrupts skeletal muscle circadian transcriptome. A. Venn diagram of AL and ZT0-4 TRF cycling genes. B. Heat map of AL unique cycling genes and TRF de-novo cycling genes. C. rAMP distribution diagram of AL and TRF cycling genes. D. Rose diagram with phase distribution of AL and TRF cycling genes. E. FPKM of AL and TRF core clock genes *Bmal1, Clock, Per1, Per2, Cry1, Cry2, Nr1d1* and *Dbp* (clock control gene), N = 3. Values represent the average ± SD. *: $P < 0.05$, **: $P < 0.01$, ***: $P < 0.001$, ****: $P < 0.0001$.

PCR, and the results were consistent with RNA-seq (Fig. S2). This result aligns with the decrease in the number of cycling genes following ZT0-4 TRF, suggesting that ZT0-4 TRF disrupts the circadian clock in muscle by inhibiting the rhythmic expression of core clock genes.

3.2. Enrichment analysis of differentially cycling genes

We conducted KEGG pathway enrichment analysis to elucidate the biological functions of cycling genes. Our results indicated that cycling genes unique to AL mice were primarily enriched in focal adhesion, regulation of actin cytoskeleton, Rap 1 signaling pathway, phospholipase D signaling pathway, protein processing in the endoplasmic reticulum, circadian rhythm, thyroid hormone signaling pathway, longevity regulating pathway, PTH synthesis, secretion, and action, vascular smooth muscle contraction, (Fig. 2A). This suggests that under normal dietary conditions, skeletal muscle exhibits robust rhythms in movement, energy metabolism, and hormone secretion. In contrast, the newly rhythmic genes induced by ZT0-4 TRF were primarily associated with phagosome, cell adhesion molecules, RNA degradation, glycolysis/gluconeogenesis, antigen processing and presentation, axon guidance, and intestinal immune network for IgA production (Fig. 2B). These findings suggest that TRF may affect the rhythmicity in glucose metabolism, nerve system and immune response.

Collectively, these results imply that ZT0-4 TRF leads to circadian reprogramming in skeletal muscle, thereby facilitating adaptations in muscle function to cope with an altered dietary environment.

3.3. Enrichment analysis of TRF-induced differentially expressed genes

To further probe the effects of ZT0-4 on muscle, we examined differentially expressed genes (DEGs) at four time points: CT1, CT7, CT13, and CT19. Our analysis identified 82, 153, 224, and 109 DEGs at these time points, totaling 389 genes (Fig. 3A). Among these, only 18 genes were consistently differentially expressed at all four time points (Fig. 3B). Of these 18 DEGs, except for rhythmically expressed genes *Nr1d1* and *Agap1*, which exhibited significant phase shifts after TRF, the expression of other genes significantly increased or decreased across the four time points (Fig. 3C). Notably, TRF led to a substantial upregulation in the expression of *Actc1, Mybph,* and *Myl9* compared with AL mice, which are positive regulatory genes associated with muscle growth and contraction, while the expression of negative regulatory genes *Fbxo32* and *Mrln*, linked to muscle atrophy, decreased significantly in TRF mice (Fig. 3C).

Furthermore, we conducted a differential expression analysis on samples from all AL mice (n = 12) and TRF mice (n = 12) at various time points. Compared with AL mice, ZT0-4 TRF induced 151 upregulated genes and 50 downregulated genes (Fig. 3D). Pathway analysis revealed that DEGs were enriched in processes related to cellular senescence, AMPK signaling pathway, biosynthesis of unsaturated fatty acids, and insulin signaling (Fig. 3E). The upregulation of DEGs associated with cell proliferation, AMPK signaling, and unsaturated fatty acid synthesis (Fig. 3F), along with the changes in genes related to muscle growth and insulin signaling (Fig. 3C), suggests that ZT0-4 TRF may impact muscle plasticity and insulin sensitivity.

3.4. TRF induces muscle fiber remodeling in mice

Skeletal muscle is a remarkably adaptable tissue capable of responding to external nutritional signals and undergoing structural remodeling [25,26]. First, we detected no significant difference in the weight of the gastrocnemius muscle of ZT0-4 TRF mice compared with the AL group (Fig. 4A). To further confirm the impact of ZT0-4 TRF on muscle plasticity, we conducted an analysis of muscle fiber type proportions. Two weeks after TRF, we observed an elevated expression of the type II muscle fiber biomarker *Myh2*

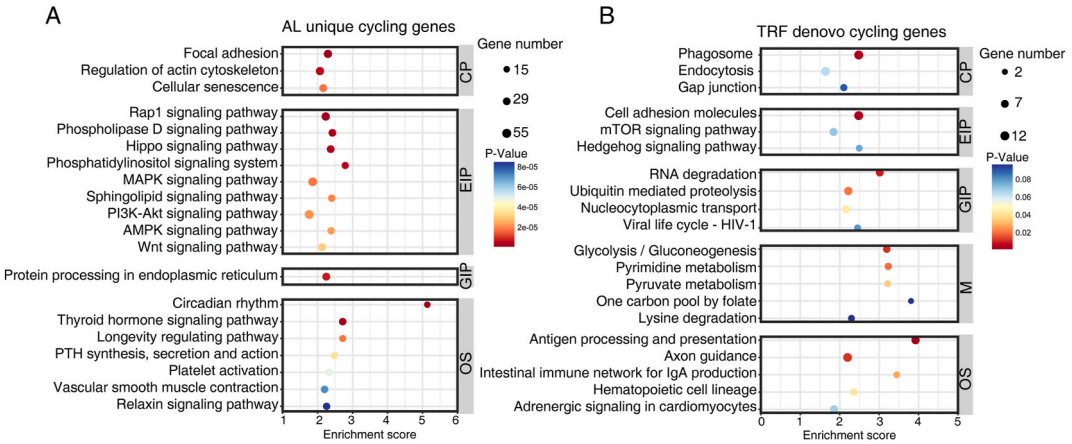

Fig. 2. KEGG enrichment of AL unique cycling genes and TRF de-novo cycling genes. Enrichment analysis of the KEGG pathway of A. AL unique cycling genes and B. ZT0-4 TRF de-novo cycling genes. (CP: Cellular Processes, EIP: Environmental Information Processing, GIP: Genetic Information Processing, M: Metabolism, OS: Organismal Systems).

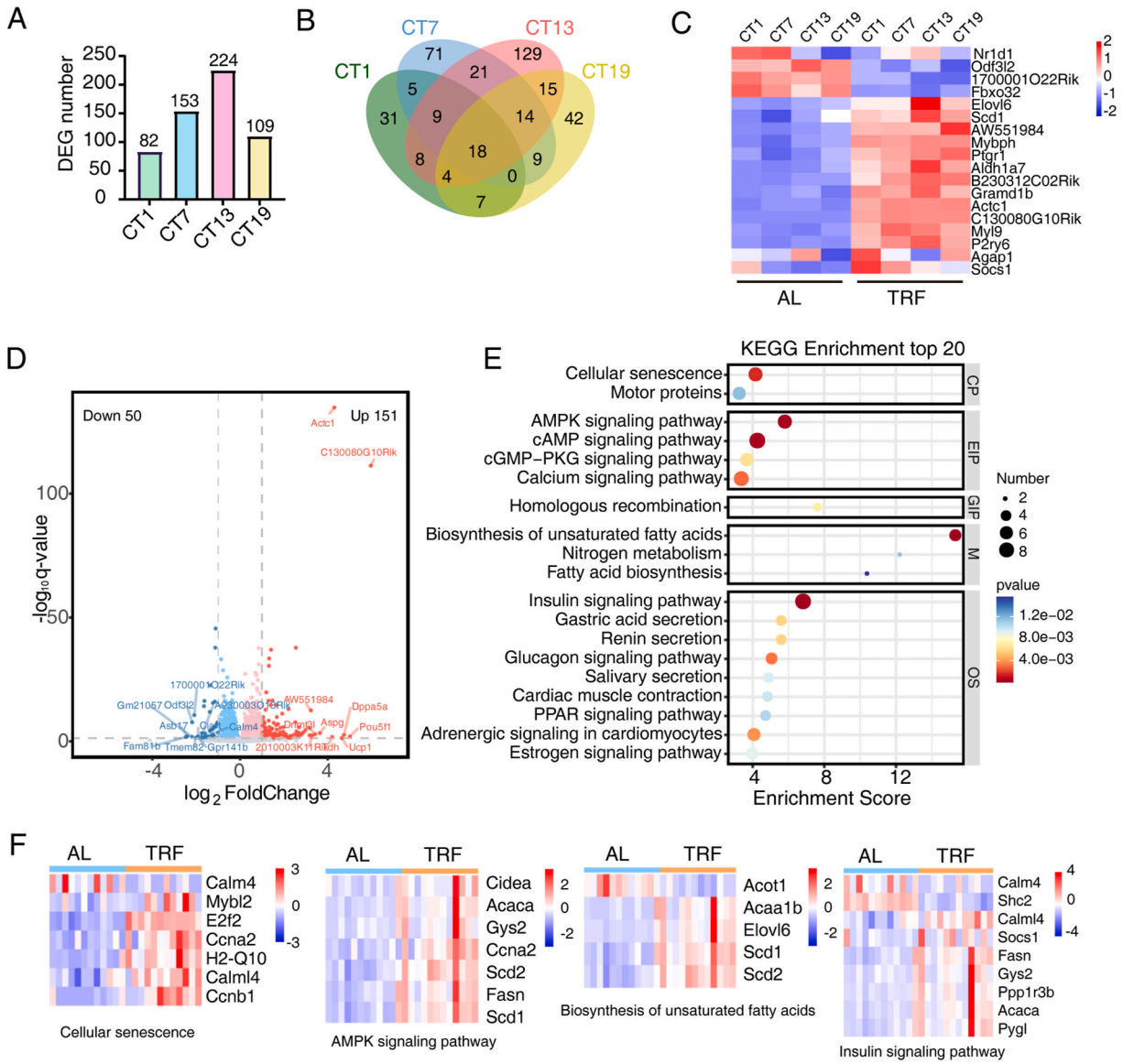

Fig. 3. Analysis of differentially expressed genes in AL and TRF muscles. A. Statistics of CT1, CT7, CT13, and CT19 DEGs (N = 3). B. Venn diagram of CT1, CT7, CT13, and CT19 DEGs. C. Gene expression heat map of 18 common DEGs. D. Volcano plot of DEGs (N = 12). E. KEGG pathway enrichment analysis of all DEGs. F. Heat map of gene expression related to signaling pathways predominantly enriched in AL and TRF DEGs.

(IIa) compared with AL mice, while the expression of *Myh1* (IIx), *Myh4* (IIb) and type I muscle fiber biomarker *Myh7* showed no significant difference (Fig. 4B). We further verified this result by detecting the expression of MYH1, MYH2, MYH4 and MYH7 at protein levels in muscle samples collected at ZT6 after TRF procedure (Fig. 4C and D).

The above results suggest that TRF may increase the proportion of type II myofibers in the gastrocnemius muscle. We then used MYH7 immunofluorescence to detect type I myofibers in the gastrocnemius muscle, and the results showed that type I myofibers were significantly reduced in TRF mice compared with AL mice (Fig. 4E and F). The proportion of type IIb myofibers, which accounts for the highest proportion in the gastrocnemius muscle, did not change significantly between the two groups (Figs. S3A and S3B), suggesting that the proportion of IIa myofibers and IIx myofibers increased in the gastrocnemius muscle of TRF mice. In addition, we also examined the proportion of type I myofibers in the soleus muscle, and the results showed that compared with AL mice, the proportion of type I myofibers in the soleus of TRF mice also decreased significantly (Fig. 4G and H).

In summary, these results imply that TRF has the potential to induce muscle fiber remodeling, thereby affecting muscle motor function.

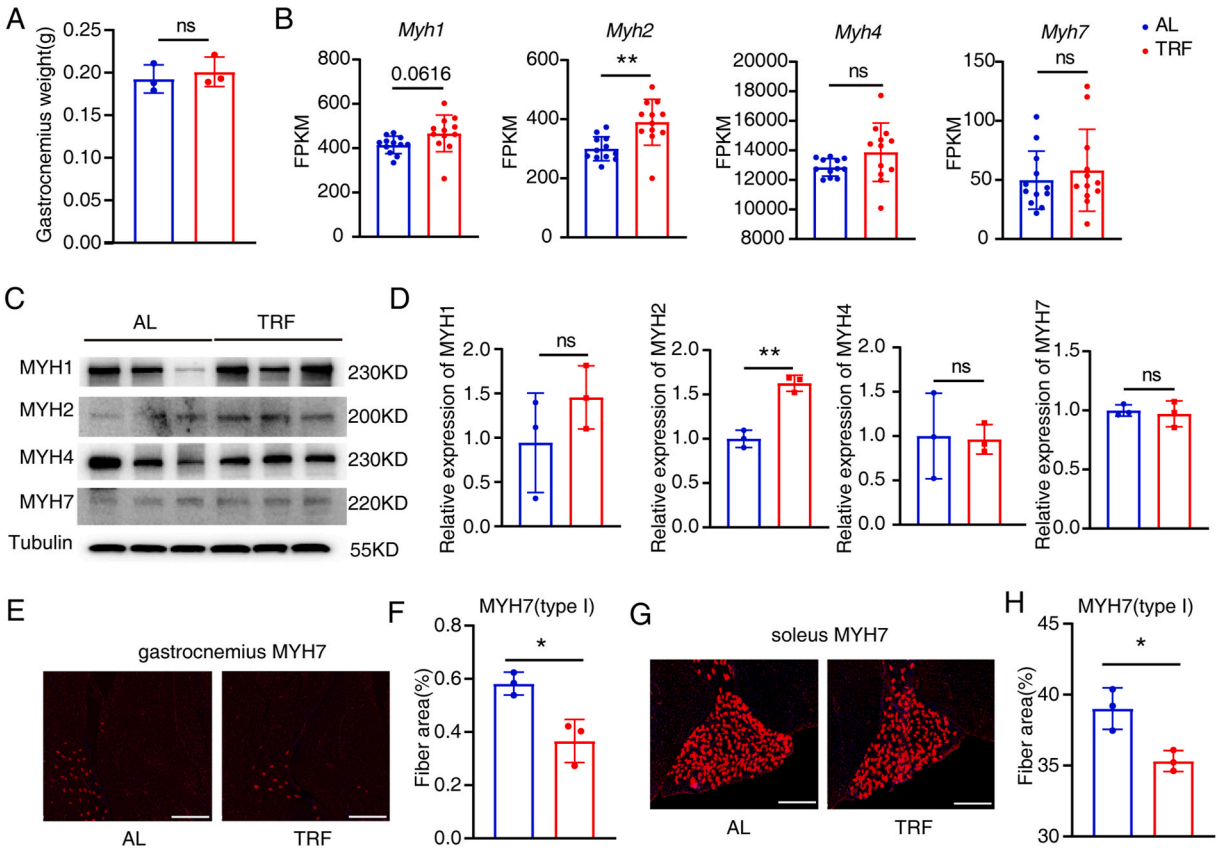

Fig. 4. Effects of TRF on skeletal muscle fiber types. A. Gastrocnemius muscle weight of AL and TRF mice. B. FPKM of AL and TRF type II muscle fiber biomarkers *Myh1*, *Myh2, Myh4* and type I muscle fiber *Myh7* (N = 12). C. Western blot of MYH1, MYH2, MYH4 and MYH7 in gastrocnemius of AL and TRF mice collected in ZT6 (N = 3). Refer to the Supplementary File 1 for full scans of blots. D. Statistics of MYH1, MYH2, MYH4 and MYH7 protein expression. E. Immunofluorescence of MYH7 in AL and TRF gastrocnemius muscle (N = 3, Scale bar: 500 μm). F. Statistics of the fiber area in gastrocnemius muscle. G. Immunofluorescence of MYH7 in AL and TRF soleus muscle (N = 3, Scale bar: 500 μm). H. Statistics of the fiber area in soleus muscle. Values represent the average ± SD. *: $P < 0.05$, **: $P < 0.01$, ns: not significant.

3.5. TRF induces insulin resistance in mice

Skeletal muscle plays a pivotal role in insulin-mediated glucose uptake. To investigate the impact of TRF on glucose metabolism, we conducted insulin tolerance tests (ITT) and glucose tolerance tests (GTT) after two weeks of ZT0-4 TRF in mice. The food intake of TRF mice was significantly lower than that of AL mice in the first eight days. However, by the ninth day, the food intake became consistent with that of the AL group (Fig. 5A). The body weight of mice did not differ significantly between AL and TRF mice (Fig. 5B). The ITT results demonstrated a significant reduction in the insulin sensitivity of mice following TRF, with a mild but statistically insignificant glucose intolerance observed in the TRF group (Fig. 5C–F). To further explore whether the insulin sensitivity of the muscle changes after TRF, we detected the activation of the AKT signaling pathway in the gastrocnemius muscle of AL and TRF mice before and after insulin injection. The results showed that insulin injection can significantly promote the phosphorylation of AKT in the gastrocnemius muscle of AL mice (Fig. 5G and H). We also found the phosphorylation of AKT in TRF mice increased significantly, but the degree of increase was significantly lower than that in AL mice (Fig. 5G and H) ，suggesting an impaired insulin response sensitivity in muscle of TRF mice.

These findings indicate that while ZT0-4 TRF has the potential to promote muscle remodeling, it also carries the adverse effect of inducing insulin resistance.

3.6. No significant effect of TRF on bone quality in mice

Specific deletion of *Bmal1* in muscle has been shown to result in the thickening of the distal tibia, increased calcaneal tendon calcification, and reduced ankle cartilage [18], suggesting the involvement of the muscle molecular circadian clock in the regulation of bone metabolism. In our study, we found that ZT0-4 TRF disrupts the skeletal muscle clock and damps the circadian expression of core clock genes *Bmal1* and *Clock*. To assess its impact on bone, we conducted micro-CT analysis on the femoral tissue of mice subjected to AL, ZT0-4 TRF, and ZT12-16 TRF. Our results indicated that neither two weeks of ZT0-4 TRF nor ZT12-16 TRF (with ZT12-16 matching

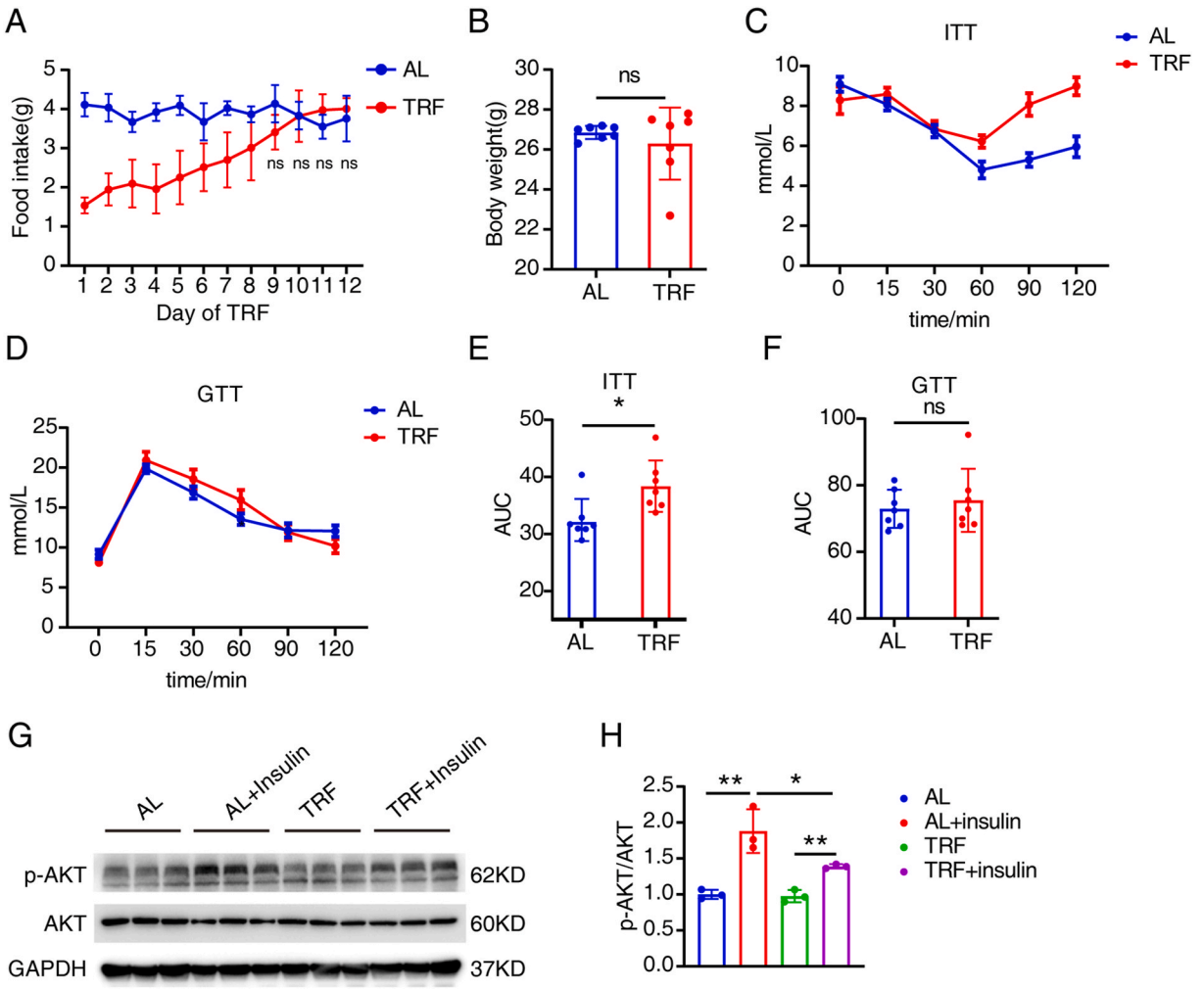

Fig. 5. TRF induces insulin resistance. A. Food intake of AL and TRF mice. B. Body weight of AL and TRF mice before fasting. C. ITT curve of AL and TRF mice. D. GTT curve of AL and TRF mice. E-F. Statistics of the area under curve (AUC) of ITT and GTT in AL and TRF mice. G. Western blot of AKT, p-AKT and GAPDH in gastrocnemius of AL and TRF mice before and 30 min after insulin injection (N = 3). Refer to the Supplementary File 1 for full scans of blots. H. Statistics of p-AKT/AKT protein expression. Values represent the average ± SD. *: $P < 0.05$, **: $P < 0.01$, ns: not significant.

the phase of the normal feeding time in mice) had a significant impact on cortical bone density and thickness, cancellous bone mineral density (BMD), BV/TV, trabecular thickness, number, or space (Fig. 6A–C). These findings suggest that short-term TRF may not have notable adverse effects on bone quality in mice.

4. Discussion

Our earlier investigation revealed that, compared to TRF implemented during other time windows, ZT0-4 TRF had a more pronounced effect on altering mouse wheel-running rhythms - a classic indicator of circadian clock output. This effect was demonstrated by an extension of the time span from the onset of activity to activity, which remained observable for four weeks under both LD and DD conditions after returning to AL. Conversely, the after-effects of TRF during other phases dissipated upon the return to AL [20], highlighting the significant impact of ZT0-4 TRF on the circadian clock. This is in line with findings by Kelly et al., who investigated the effects of daytime feeding (8:00–19:00) and delayed feeding (12:00–21:00) on body weight and metabolism in individuals with a normal BMI. They discovered that delayed feeding increased body weight and induce insulin resistance [27], consistent with our observation of ZT0-4 TRF promoting insulin resistance in mice. In older, metabolically compromised men, the insulin sensitivity was reduced compared with young, healthy men [28]. The aging of skeletal muscle is often accompanied by a weakening of the biological clock, including a decrease in the number and amplitude of rhythmic genes [29], which also suggests that the disruption of the skeletal muscle biological clock may be related to the development of insulin resistance.

By comparing the expression phase of core clock genes in skeletal muscle of humans and mice, we found that the phase of expression of core clock genes in skeletal muscle is consistent with the phase of activity, so the biological clock of skeletal muscle may

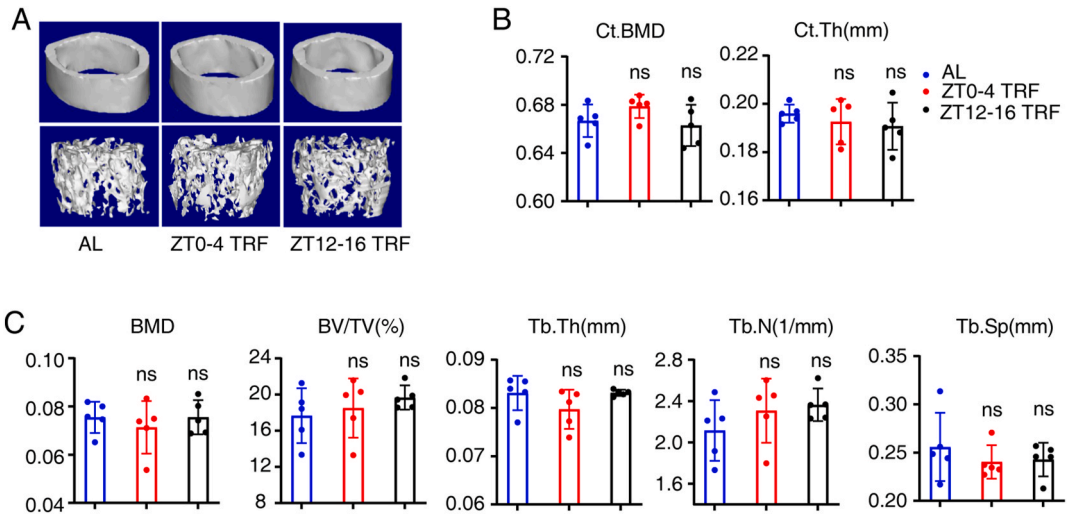

Fig. 6. Effect of ZT0-4 TRF on bone mass in mice. A. Three-dimensional reconstruction of cortical bone and cancellous bone in AL, ZT0-4, ZT12-16 TRF mice. B. Statistical results of cortical bone density and thickness in AL, ZT0-4, and ZT12-16 TRF mice (N = 5). C. Statistical results of BMD, bone volume fraction (BV/TV), trabecular bone thickness (Tb. Th), trabecular bone number (Tb. N), trabecular bone gap (Tb. sp) in AL, ZT0-4, and ZT12-16 TRF mice (N = 5). Values represent the average ± SD. ns: not significant.

be more regulated by activity [30]. Although the rhythmic phase of SCN neuronal activity in humans and mice is completely opposite, signals from the SCN do not cause significant changes in the skeletal muscle core clock. Therefore, in skeletal muscle research, ZT0-4 TRF is akin to late-night eating in humans. Consequently, exploring the impact of ZT0-4 TRF on the skeletal muscle system may provide valuable insights into the regulation of skeletal muscle homeostasis influenced by late-night eating behavior.

ZT0-4 TRF disrupts the muscle clock, leading to a near disappearance of the rhythmic expression of core clock genes, including *Bmal1, Clock, Cry1,* and *Cry2*. This outcome aligns with data from previous studies on ZT1-11 TRF over 5 weeks and ZT0-12 TRF over 8 weeks or 3 weeks [31–33]. They also found that, unlike muscle tissue, daytime TRF can induce 6–12 h shift in the peak diurnal expression of genes in liver. One recent study found that TRF during the inactive phase can abolish the daily rhythm in mitochondrial respiration in rat skeletal muscle [34]. This finding also supports our conclusion that light phase TRF disrupts the biological rhythm of skeletal muscle. Besides, Manella et al. found that clocks in different tissues largely differed in their response to daytime TRF, from phase inversion to no response or even loss of rhythmicity through a daytime TRF [35]. These results suggest that different organs respond differently to nutrition signals. Since muscle contraction influences clock gene expression in skeletal muscle through a calcium-dependent pathway [36], we speculated that the effect of ZT0-4 TRF on the activity rhythm of mice (the activity time span increased by 2.5 h (Fig. S1)) might damp the skeletal muscle circadian clock through muscle contraction. One research also found that high-fat feeding does not disrupt daily rhythms in female mice because of protection by estrogen [37], indicating a sex difference in response to nutrition signal. Thus, whether ZT0-4 TRF can affect the skeletal muscle circadian clock in female mice needs further exploration.

Although ZT0-4 TRF disrupts the rhythmic expression of core clock genes, it also induces the rhythmic expression of numerous genes, with immune system-related pathways being the most enriched. Previous research has shown that 12-h TRF can alter the innate immune response to bacterial endotoxins in mice [38]. They found that daytime TRF can enhance the immune response level of mice during the inactive period and reduce the immune response level of mice during the active period, while night-time TRF can enhance the immune response level of mice during the active period. Another human study has demonstrated that 12 weeks of 12-h antiphase TRF (12 h of fasting during the daytime) can reduce the total count of white blood cells, lymphocytes, neutrophils, and natural killer cells [39], suggesting that the immune system is responsive to dietary nutritional signals. In this study, cycling genes analysis of RNA-seq data sampled at a 6-h time interval may cause certain false positives. The accuracy of the results can be increased through higher-density sampling. Here, we overlapped the results of both RAIN and Metacycle to identify cycling genes, and the disappearance of rhythmic expression in core clock genes of AL mice following TRF can be observed, demonstrating the relative reliability of employing this analytical method to study rhythmic genes.

Through the analysis of DEGs, we observed that the number of DEGs also followed arhythmic pattern. In this study, only 18 common DEGs were identified at all four sampling time points. Therefore, DEG analysis of samples from different time points may lead to different conclusions. KEGG enrichment analysis revealed that pathways related to cell cycle, cellular senescence, the AMPK pathway, and unsaturated fatty acid synthesis were enriched. During the low-energy state following exercise, the AMPK signaling pathway is activated, promoting processes such as fatty acid oxidation, mitochondrial biogenesis, mitophagy, and gene transcription through glucose and fatty acid uptake [40]. This in turn facilitates skeletal muscle adaptation to exercise. Notably, the activity of mice increased significantly during the initial 1–2 h of TRF, a phenomenon referred to as food anticipatory activity (FAA) [41]. This FAA was also observed in ZT0-4 TRF [20]. Consequently, the low-energy state following FAA may be associated with AMPK activation. Several studies have demonstrated that unsaturated fatty acid synthesis can prevent muscle loss, inhibit protein degradation, and improve

muscle morphology and function [42].

Skeletal muscle-specific deletion of *Bmal1* in mice has been shown to increase activity and muscle mass, but decrease muscle strength and the proportion of type II muscle fibers [17]. In vitro studies have demonstrated that *Bmal1* can promote myogenic differentiation of C2C12 cells [43]. Our investigation indicates that ZT0-4 TRF can enhance the expression of muscle growth-related genes *Actc1, Mybph,* and *Myl9*, inhibit the expression of negative regulators of muscle atrophy, such as *Fbxo32*, and increase the proportion of type II muscle fibers. The effects on muscle growth-related genes and myofiber remodeling induced by TRF may be attributed to the suppressed expression of *Bmal1*. A recent study by Xin et al. reported that TRF lasting for 3 weeks and restricting eating to 12 h of the day/sleep time increased the proportion of SDH-positive IIA muscle fibers, decreased the proportion of GPDH-positive IIx muscle fibers, and enhanced the running endurance of mice without exercise [44]. In our study, we also observed that 2 weeks of TRF extending for 4 h could promote muscle fiber remodeling. However, the expression of genes *Myh2* and *Myh1*, encoding MyHC-IIa and MyHC-IIx, was up-regulated after TRF, which differs from Xin et al.'s findings. This variation may be related to differences in the phase, duration of the feeding window, and days of TRF intervention. In aged monkeys, caloric restriction increased the proportion of type II and mixed myofibers compared with controls, while type I fibers remained unaffected [45]. We also found that during the ZT0-4 TRF adaptation process, the food intake of mice was significantly lower than the normal food intake in the first 8 days. Thus, the caloric restriction during the TRF adaptation phase may lead to the remodeling of myofibers. It is reported that type I myofibers are rich in myoglobin (MB), triglycerides, mitochondria and capillary. They have a greater insulin sensitivity than type IIb fibers [9]. Therefore, the decreased insulin sensitivity of mice caused by ZT0-4 TRF may also be related to the increase of type IIb fibers. Since ZT0-4 TRF also changes the circadian clocks of other peripheral tissues that regulate insulin sensitivity, such as the liver and adipose tissue [46], the weakening of insulin sensitivity caused by TRF may not only be related to the damping of the skeletal muscle circadian clock.

There is evidence that people with circadian clock disruption due to shift work and sleep disorders have a higher risk of osteoporosis [47–49]. And constant light exposure reduced skeletal muscle function, caused trabecular bone deterioration, and induced a transient pro-inflammatory state in mice [50]. Therefore, environmentally induced disturbance of the body's biological clock is a risk factor leading to the destruction of bone health. In healthy, non-obese adults, 8-h time-restricted diet has no significant effect on BMD [51]. Two randomized controlled trials investigated the effects of 8-h TRF for 12 weeks in overweight and obese adults. Lowe et al. found that the TRF group tended to have an increase in total body BMC [52]. Lobene et al. reported a greater P1NP reduction in the bone formation marker P1NP in the control group than TRF group, indicating a protective response of TRF in bone mass [53]. However, it is not clear whether TRF before bedtime causes rhythm disorders and bone metabolism damage. Therefore, we examined the effect of TRF on bone quality but found no significant differences. This may be attributed to the relatively short duration of our TRF experiments (2 weeks). Given that *Bmal1* deletion in skeletal muscle can induce premature aging and abnormal calcification [18], we believe that longer ZT0-4 TRF will reduce bone mass and affect the microstructure of trabecular bone in mice, which requires further confirmation in our future work.

In summary, our study found in mice that TRF before sleep can disrupt skeletal muscle circadian rhythms and reprogram the skeletal muscle rhythm signaling pathways. And ZT0-4 TRF can also promote skeletal muscle fiber remodeling with the side effects such as insulin resistance and other metabolic consequences.

Funding

This work was supported by grants from the Quzhou Science and Technology Research Project (2023K107) to Q.Z and (2021Y005) Z.Y, Pre-research Fund of the Second Affiliated Hospital of Soochow University (SDFEYJBS2108) to Q.Z.

Data availability statement

Sequence data from this article have been deposited with the NCBI SRA Data Libraries under Accession No: PRJNA1124862.

CRediT authorship contribution statement

Zhou Ye: Writing – original draft, Project administration, Funding acquisition. **Kai Huang:** Project administration. **Xueqin Dai:** Project administration. **Dandan Gao:** Project administration. **Yue Gu:** Formal analysis, Data curation. **Jun Qian:** Formal analysis, Data curation. **Feng Zhang:** Writing – review & editing, Validation. **Qiaocheng Zhai:** Writing – review & editing, Funding acquisition, Conceptualization.

Declaration of competing interest

The authors declare that they have no known competing financial interests or personal relationships that could have appeared to influence the work reported in this paper.

Appendix A. Supplementary data

Supplementary data to this article can be found online at https://doi.org/10.1016/j.heliyon.2024.e37475.

References

[1] M.H. Hastings, E.S. Maywood, M. Brancaccio, Generation of circadian rhythms in the suprachiasmatic nucleus, Nat. Rev. Neurosci. 19 (8) (2018) 453–469.
[2] J.S. Takahashi, Transcriptional architecture of the mammalian circadian clock, Nat. Rev. Genet. 18 (3) (2017) 164–179.
[3] A. Zarrinpar, A. Chaix, S. Panda, Daily eating patterns and their impact on health and disease, Trends Endocrinol. Metabol. 27 (2) (2016) 69–83.
[4] M. Hatori, et al., Time-restricted feeding without reducing caloric intake prevents metabolic diseases in mice fed a high-fat diet, Cell Metabol. 15 (6) (2012) 848–860.
[5] A. Chaix, et al., Time-restricted feeding is a preventative and therapeutic intervention against diverse nutritional challenges, Cell Metabol. 20 (6) (2014) 991–1005.
[6] J.Y. Tsai, et al., Influence of dark phase restricted high fat feeding on myocardial adaptation in mice, J. Mol. Cell. Cardiol. 55 (2013) 147–155.
[7] S. Gill, et al., Time-restricted feeding attenuates age-related cardiac decline in Drosophila, Science 347 (6227) (2015) 1265–1269.
[8] J.E. Villanueva, et al., Time-restricted feeding restores muscle function in Drosophila models of obesity and circadian-rhythm disruption, Nat. Commun. 10 (1) (2019) 2700.
[9] E.F. Sutton, et al., Early time-restricted feeding improves insulin sensitivity, blood pressure, and oxidative stress even without weight loss in men with prediabetes, Cell Metabol. 27 (6) (2018) 1212–1221 e3.
[10] E.N.C. Manoogian, et al., Feasibility of time-restricted eating and impacts on cardiometabolic health in 24-h shift workers: the Healthy Heroes randomized control trial, Cell Metabol. 34 (10) (2022) 1442–1456 e7.
[11] U. Albrecht, Timing to perfection: the biology of central and peripheral circadian clocks, Neuron 74 (2) (2012) 246–260.
[12] F. Damiola, et al., Restricted feeding uncouples circadian oscillators in peripheral tissues from the central pacemaker in the suprachiasmatic nucleus, Genes Dev. 14 (23) (2000) 2950–2961.
[13] E. Maury, K.M. Ramsey, J. Bass, Circadian rhythms and metabolic syndrome: from experimental genetics to human disease, Circ. Res. 106 (3) (2010) 447–462.
[14] K. Oishi, C. Hashimoto, Short-term time-restricted feeding during the resting phase is sufficient to induce leptin resistance that contributes to development of obesity and metabolic disorders in mice, Chronobiol. Int. 35 (11) (2018) 1576–1594.
[15] K.K. Baskin, B.R. Winders, E.N. Olson, Muscle as a "mediator" of systemic metabolism, Cell Metabol. 21 (2) (2015) 237–248.
[16] F. Hontoir, et al., Age-related morphometric changes of the tidemark in the ovine stifle, Anat. Histol. Embryol. 48 (4) (2019) 366–374.
[17] K.A. Dyar, et al., Muscle insulin sensitivity and glucose metabolism are controlled by the intrinsic muscle clock, Mol. Metabol. 3 (1) (2014) 29–41.
[18] E.A. Schroder, et al., Intrinsic muscle clock is necessary for musculoskeletal health, J. Physiol. 593 (24) (2015) 5387–5404.
[19] V. Acosta-Rodriguez, et al., Circadian alignment of early onset caloric restriction promotes longevity in male C57BL/6J mice, Science 376 (6598) (2022) 1192–1202.
[20] Q. Zhai, et al., Time-restricted feeding entrains long-term behavioral changes through the IGF2-KCC2 pathway, iScience 25 (5) (2022) 104267.
[21] P.F. Thaben, P.O. Westermark, Detecting rhythms in time series with RAIN, J. Biol. Rhythm. 29 (6) (2014) 391–400.
[22] G. Wu, et al., MetaCycle: an integrated R package to evaluate periodicity in large scale data, Bioinformatics 32 (21) (2016) 3351–3353.
[23] J.A. Davis, et al., High-fat and high-sucrose diets impair time-of-day differences in spatial working memory of male mice, Obesity 28 (12) (2020) 2347–2356.
[24] K.C. Kalafut, et al., Short-term ketogenic diet induces a molecular response that is distinct from dietary protein restriction, Front. Nutr. 9 (2022) 839341.
[25] K.N.a.A. Tsutaki, Regulatory mechanisms of muscle fiber types and their possible interactions with external nutritional stimuli, The Journal of Physical Fitness and Sports Medicine 1 (4) (2012) 655–664.
[26] W. Chen, et al., DHA alleviates diet-induced skeletal muscle fiber remodeling via FTO/m(6)A/DDIT4/PGC1alpha signaling, BMC Biol. 20 (1) (2022) 39.
[27] K.C. Allison, et al., Prolonged, controlled daytime versus delayed eating impacts weight and metabolism, Curr. Biol. 31 (3) (2021) 650–657 e3.
[28] J.F. Harmsen, et al., Divergent remodeling of the skeletal muscle metabolome over 24 h between young, healthy men and older, metabolically compromised men, Cell Rep. 41 (11) (2022) 111786.
[29] C.A. Wolff, et al., Defining the age-dependent and tissue-specific circadian transcriptome in male mice, Cell Rep. 42 (1) (2023) 111982.
[30] M.A. Gutierrez-Monreal, et al., Ticking for metabolic health: the skeletal-muscle clocks, Obesity 28 (Suppl 1) (2020) S46–S54. Suppl 1.
[31] P. de Goede, et al., Differential effects of diet composition and timing of feeding behavior on rat brown adipose tissue and skeletal muscle peripheral clocks, Neurobiol Sleep Circadian Rhythms 4 (2018) 24–33.
[32] A.L. Opperhuizen, et al., Feeding during the resting phase causes profound changes in physiology and desynchronization between liver and muscle rhythms of rats, Eur. J. Neurosci. 44 (10) (2016) 2795–2806.
[33] J. Reznick, et al., Altered feeding differentially regulates circadian rhythms and energy metabolism in liver and muscle of rats, Biochim. Biophys. Acta 1832 (1) (2013) 228–238.
[34] P. de Goede, et al., Time-restricted feeding during the inactive phase abolishes the daily rhythm in mitochondrial respiration in rat skeletal muscle, Faseb. J. 36 (2) (2022) e22133.
[35] G. Manella, et al., The liver-clock coordinates rhythmicity of peripheral tissues in response to feeding, Nat. Metab. 3 (6) (2021) 829–842.
[36] L. Small, et al., Contraction influences Per2 gene expression in skeletal muscle through a calcium-dependent pathway, J. Physiol. 598 (24) (2020) 5739–5752.
[37] B.T. Palmisano, J.M. Stafford, J.S. Pendergast, High-fat feeding does not disrupt daily rhythms in female mice because of protection by ovarian hormones, Front. Endocrinol. 8 (2017) 44.
[38] Y.M. Cisse, et al., Time-restricted feeding alters the innate immune response to bacterial endotoxin, J. Immunol. 200 (2) (2018) 681–687.
[39] M. Gasmi, et al., Time-restricted feeding influences immune responses without compromising muscle performance in older men, Nutrition 51–52 (2018) 29–37.
[40] R. Mounier, et al., Expanding roles for AMPK in skeletal muscle plasticity, Trends Endocrinol. Metabol. 26 (6) (2015) 275–286.
[41] R.E. Mistlberger, Circadian food-anticipatory activity: formal models and physiological mechanisms, Neurosci. Biobehav. Rev. 18 (2) (1994) 171–195.
[42] C. Lipina, H.S. Hundal, Lipid modulation of skeletal muscle mass and function, J Cachexia Sarcopenia Muscle 8 (2) (2017) 190–201.
[43] S. Chatterjee, et al., Brain and muscle Arnt-like 1 is a key regulator of myogenesis, J. Cell Sci. 126 (Pt 10) (2013) 2213–2224.
[44] H. Xin, et al., Daytime-restricted feeding enhances running endurance without prior exercise in mice, Nat. Metab. 5 (7) (2023) 1236–1251.
[45] T.W. Rhoads, et al., Molecular and functional networks linked to sarcopenia prevention by caloric restriction in rhesus monkeys, Cell Syst 10 (2) (2020) 156–168 e5.
[46] D.J. Stenvers, et al., Circadian clocks and insulin resistance, Nat. Rev. Endocrinol. 15 (2) (2019) 75–89.
[47] D. Feskanich, S.E. Hankinson, E.S. Schernhammer, Nightshift work and fracture risk: the nurses' health study, Osteoporos. Int. 20 (4) (2009) 537–542.
[48] I. Quevedo, A.M. Zuniga, Low bone mineral density in rotating-shift workers, J. Clin. Densitom. 13 (4) (2010) 467–469.
[49] N. Sasaki, et al., Impact of sleep on osteoporosis: sleep quality is associated with bone stiffness index, Sleep Med. 25 (2016) 73–77.
[50] E.A. Lucassen, et al., Environmental 24-hr cycles are essential for health, Curr. Biol. 26 (14) (2016) 1843–1853.
[51] C.R. Martens, et al., Short-term time-restricted feeding is safe and feasible in non-obese healthy midlife and older adults, Geroscience 42 (2) (2020) 667–686.
[52] D.A. Lowe, et al., Effects of time-restricted eating on weight loss and other metabolic parameters in women and men with overweight and obesity: the TREAT randomized clinical trial, JAMA Intern. Med. 180 (11) (2020) 1491–1499.
[53] A.J. Lobene, et al., Time-restricted eating for 12 Weeks does not adversely alter bone turnover in overweight adults, Nutrients 13 (4) (2021).